Numerical Simulations of Airflows and Tracer Transport in the Southwestern United States

TETSUJI YAMADA

Yamada Science and Art Corporation, Santa Fe, New Mexico

(Manuscript received 18 May 1998, in final form 24 November 1998)

ABSTRACT

Project MOHAVE (Measurement of Haze and Visual Effects) produced a unique set of tracer data over the southwestern United States. During the summer of 1992, a perfluorocarbon tracer gas was released from the Mohave Power Project (MPP), a large coal-fired facility in southern Nevada. Three-dimensional atmospheric models, the Higher-Order Turbulence Model for Atmospheric Circulation–Random Puff Transport and Diffusion (HOTMAC–RAPTAD), were used to simulate the concentrations of tracer gas that were observed during a portion of the summer intensive period of Project MOHAVE. The study area extended from northwestern Arizona to southern Nevada and included Lake Mead, the Colorado River Valley, the Grand Canyon National Park, and MPP. The computational domain was 368 km in the east–west direction by 252 km in the north–south direction. Rawinsonde and radar wind profiler data were used to provide initial and boundary conditions to HOTMAC simulations. HOTMAC with a horizontal grid spacing of 4 km was able to simulate the diurnal variations of drainage and upslope flows along the Grand Canyon and Colorado River Valley. HOTMAC also captured the diurnal variations of turbulence, which played important roles for the transport and diffusion simulations by RAPTAD. The modeled tracer gas concentrations were compared with observations. The model's performance was evaluated statistically.

1. Introduction

Visibility impairment in the Grand Canyon and other national parks in the southwestern United States has captured the attention of federal agencies, local society, and environmental groups. Project MOHAVE (Measurement of Haze and Visual Effects; Pitchford et al. 1997) was designed to estimate the magnitude and frequency of visibility impairment at the Grand Canyon National Park (GCNP). A comprehensive field campaign was conducted during the summer of 1992. The study area included Las Vegas, Nevada, at the northwest corner; Page, Arizona, at the northeast corner; and the Mohave Power Project (MPP) along the south boundary. MPP, a large coal-fired facility in southern Nevada, is located approximately 20 km south of Cottonwood Cove, a town west of Lake Mohave along the California and Nevada state boundary. GCNP was centered in the study area.

Meteorological data were collected by using rawinsondes and radar wind profilers for upper-air soundings and tower instrumentations for surface-layer measurements. To understand transport and diffusion processes in the study area, a perfluorocarbon tracer gas, orthoperfluorodimethylcyclohexane (oPDCH), was released from MPP.

Previous modeling studies were conducted prior to the release of the tracer data. In other words, it was a blind test. Modeling results unfortunately were not satisfactory (Green 1997). Since we did not participate in the initial modeling studies, we were not familiar with the issues associated with the modeling deficiencies. Based on the current study and discussions with the modelers who participated in the initial modeling studies, we now speculate that some causes for the poor performance might have been that a coarse grid spacing (12 km) was used or that large-scale weather variations were not included.

For the current study, the tracer data were available for model performance evaluation. The tracer data were useful to avoid obvious mistakes (such as misreading emission rates, concentration units, or sampling duration), which would be detected easily by comparing the model results with observations. It was important to obtain realistic wind, turbulence, and tracer concentration distributions by checking the model results with observations, because other scientists are going to use the modeled results for their atmospheric chemistry computations.

In this study, the three-dimensional atmospheric modeling system Higher-Order Turbulence Model for At-

Corresponding author address: Dr. Tetsuji Yamada, Yamada Science and Art Corporation, Rt. 4 Box 81-A, Santa Fe, NM 87501.
E-mail: ysa@ysasoft.com

mospheric Circulation–Random Puff Transport and Diffusion (HOTMAC–RAPTAD) was used to simulate the tracer gas concentrations that were observed during a portion of the summer intensive period of Project MOHAVE. The modeled tracer surface concentrations were compared with observations.

2. Models

a. HOTMAC

HOTMAC is a three-dimensional numerical model for weather forecasting. The basic equations of HOTMAC were described in detail by Yamada and Bunker (1988, 1989); only a summary is given here. The governing equations are conservation equations for mass, momentum, potential temperature deviations, water vapor, and turbulence kinetic energy. Note that the deviations of potential temperature from the large-scale mean values were solved instead of the absolute values of potential temperature. This modification was found to be useful to reduce computational errors and to keep predicted wind fields realistic (Yamada and Bunker 1989). The magnitude of the potential temperature is about 300 K, but the deviations from the large-scale values are on the order of 10 K or less. Thus, one or two more significant figures can be carried throughout the computations if temperature deviations, instead of absolute temperatures, are used.

The current model assumes hydrostatic equilibrium and uses the Boussinesq approximation. Therefore, in theory, the model is valid for flows for which the vertical scale of the modeled system is small when compared with its horizontal scale (hydrostatic equilibrium) and for small temperature variations in the horizontal directions (Boussinesq approximation). Both assumptions are satisfied easily with the horizontal grid spacing of 4 km used in this study.

HOTMAC is based on the concept of the ensemble average: the solutions are sought in terms of mean values and deviations from the mean. An ensemble average model is a realistic choice, in terms of accuracy and computational time, for three-dimensional atmospheric simulations. Turbulence equations are based on the level-2.5 turbulence-closure model (Mellor and Yamada 1982), which also was found to be a good choice for three-dimensional simulations, in terms of the accuracy and computation time.

HOTMAC uses a statistical approach for computing the amount of condensation. This approach is very different from a conventional method in which the amount of condensation is determined simply as the excess of the grid-averaged mixing ratio of water vapor over the saturation value. The conventional method likely underestimates the amount of condensation (or clouds), because clouds do exist in the atmosphere because of fluctuations of the mixing ratio of water vapor even if the grid volume–averaged mixing ratio is less than the saturation value.

The current statistical approach considers cloud volume, which is the ratio of a volume occupied by clouds to a grid volume. The analytical relationships (Mellor 1977) indicate, for example, that the cloud volume function increases with increasing mixing ratio of water vapor and takes positive values even if the air is unsaturated. In other words, clouds can exist partially even if the mixing ratio of water vapor is not saturated when averaged over a grid volume. This existence is realistic, because the grid spacing normally used in mesoscale models is larger than the size of small clouds. Therefore, the current cloud model can use a relatively large grid spacing, which could save substantial computational time. A statistical cloud model such as the current one avoids the ambiguous condensation criteria often used by coarse-grid models, for which saturation values are lowered arbitrarily to compensate for the amount of cloud not resolved by the grids. This method has been applied to simulations of the Barbados Oceanographic and Meteorological Experiment data (Yamada and Mellor 1979) and Global Atmospheric Research Program Atlantic Tropical Experiment data (Yamada and Kao 1986).

Mesoscale models such as HOTMAC are able to forecast wind distributions associated with the pressure gradients generated in the computational domain. However, any variations produced outside the computational domain must be incorporated into mesoscale models through additional forcing terms. Variations of large-scale wind distributions were incorporated into the equations of motion through a technique referred to as ''nudging'' or ''Newtonian relaxation'' (Anthes 1974; Hoke and Anthes 1976). The terms $C_n(U_t - U)$ and $C_n(V_t - V)$ were added to the equations of motion for the east–west and north–south components, respectively. Here, C_n ($=0.0005\ s^{-1}$) is a nudging coefficient; and U_t and V_t are ''target'' wind components for the corresponding wind components U and V, respectively (Yamada and Bunker 1989). Here U_t and V_t are, in general, different from the observed wind components. The nudging method is a simple but effective way to incorporate large-scale variations into a mesoscale model.

b. RAPTAD

RAPTAD is a Lagrangian model in which a number of puffs are released at the source and in which the change with time of puff characteristics, such as the location of the center and the size and age of the puff, is computed at every time step. The basic equations of RAPTAD were described in detail by Yamada and Bunker (1988); only new features are discussed here.

The vertical velocity of a nonneutrally buoyant plume is computed from the Langevin equation of motion for a homogeneous and stationary turbulent flow. The temperature of a nonneutrally buoyant plume also is as-

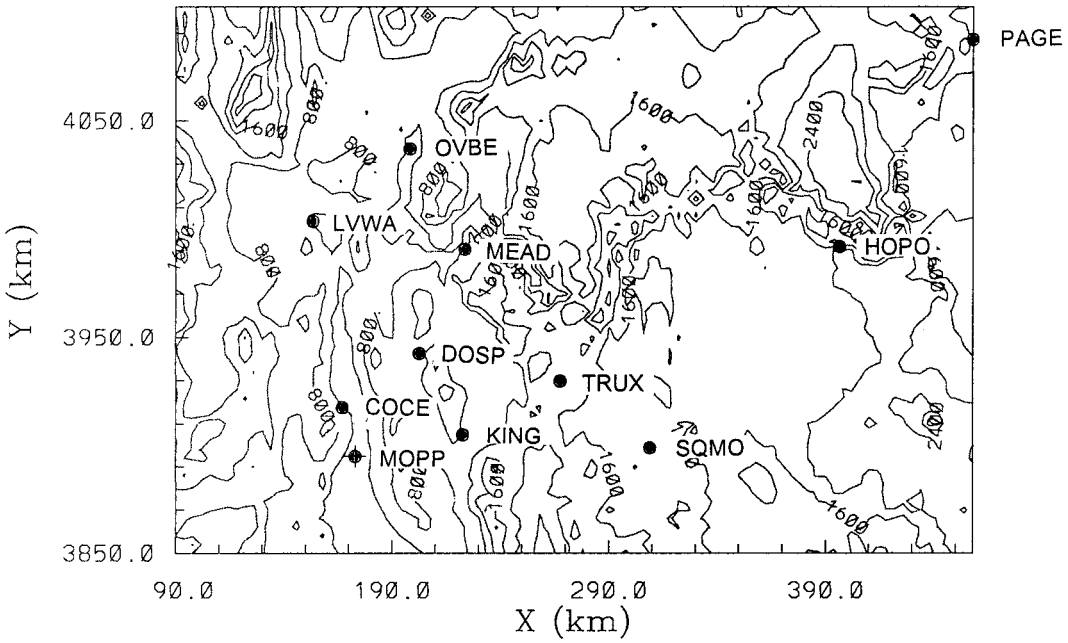

FIG. 1. The computational domain of 368 km × 252 km. Solid contour lines indicate ground elevation (m MSL), with an increment of 400 m between the contours. Locations of meteorological and sampling stations also are indicated: Mohave Power Project (MPP), Kingman (KING), Dolan Springs (DOSP), Las Vegas Wash (LVWA), Overton Beach (OVBE), Meadview (MEAD), Truxton (TRUX), Squaw Mountain (SQMO), Hopi Point (HOPO), Cottonwood Cove (COCE), and Page (PAGE). Las Vegas, Nevada, is located approximately 30 km west of Las Vegas Wash (LVWA). The Grand Canyon begins at HOPO, meanders to the north and the south directions, and ends at MEAD. The Colorado River Valley runs in the north–south direction through MOPP and COCE to near LVWA.

sumed to be computed by the Langevin equation. Following Van Dop (1992), vertical velocity ($\overline{W}$), buoyancy ($\overline{B}$), and plume height ($\overline{Z}$) are computed from the following equations:

$$\frac{d\overline{W}}{dt} = -\frac{\overline{W}}{T_W} + \overline{B}, \tag{1}$$

$$\frac{d\overline{B}}{dt} = -\frac{\overline{B}}{T_B} - N^2\overline{W}, \quad \text{and} \tag{2}$$

$$\frac{d\overline{Z}}{dt} = \overline{W}, \tag{3}$$

where

$$B \equiv \frac{g}{T}(\Theta_p - \Theta_a), \tag{4}$$

$$N^2 \equiv \frac{g}{T}\frac{d\Theta_a}{dz}, \tag{5}$$

$$T_W = T_B = A(t + t_0), \tag{6}$$

$$A = 3/4, \quad \text{and} \tag{7}$$

$$t_0 = 1 \text{ s}. \tag{8}$$

The subscripts p and a in Eq. (4) indicate plume and ambient air, respectively, g is the acceleration of gravity, T is temperature, Θ is potential temperature, z is height, and t is time. Van Dop (1992) found that model results using the above equations were in good agreement with analytical solutions for buoyant plumes.

The definition of buoyancy [Eq.(4)] was restated in terms of densities instead of potential temperatures:

$$B \equiv \frac{\rho_a - \rho_p}{\rho_a}g, \tag{9}$$

where ρ_p is the puff density, and ρ_a is the ambient air density. The original application of van Dop's (VD) model was limited to buoyant plumes. As far as the methodology is concerned, however, VD should be applicable not only to buoyant plumes but also to dense gas releases.

First HOTMAC was run to generate three-dimensional distributions of winds U_i and velocity variance σ_{u_i}. The mean W used in RAPTAD for a nonneutrally buoyant plume was obtained by adding the HOTMAC velocity (W_H) and VD's velocity (W_{VD}):

$$W = W_H + W_{\text{VD}}. \tag{10}$$

3. Initial and boundary conditions

Figure 1 shows the computational domain of 368 km in the east–west direction by 252 km in the north–south

direction. The area extends from northwestern Arizona to southern Nevada, and includes Lake Mead, the Colorado River Valley, GCNP, and MPP. Las Vegas, Nevada, is located approximately 30 km west of Las Vegas Wash (LVWA) in Fig. 1. Solid contour lines indicate ground elevation in meters above mean sea level (MSL) with an increment of 400 m between the contours. Locations of meteorological and sampling stations also are indicated.

The horizontal grid spacing was 4 km, and vertical grid spacing varied with height: 4 m for the first five levels from the surface and increasing to over 500 m at the top of the computational domain, which was 5000 m above the highest elevation (3425 m MSL). A total of 93 $\times$ 64 $\times$ 26 (vertical) grid points were used. A relatively coarse horizontal grid spacing (4 km) was used because of limited computational resources. It clearly was inadequate to resolve steep slopes inside the Grand Canyon. Nevertheless, qualitative features of wind flows over complex terrain were captured, as discussed in section 4b.

Rawinsonde data from Cottonwood Cove, Dolan Springs, and Page, along with radar profiler wind data from MPP, Truxton, and Meadview (see Fig. 1 for locations), were used to provide initial and boundary conditions to HOTMAC simulations. Considerable preprocessing was required because the wind data were taken at different times and heights. For example, upper-air soundings at Cottonwood Cove and Dolan Springs were taken approximately at 0400, 1000, and 1600 MST (UTC $-$ 0700) while radar profiler data were reported hourly. Routine radiosonde soundings at Page were taken twice daily. The wind data first were interpolated to HOTMAC vertical grid levels by using a linear interpolation formula. Then, the data were interpolated in the horizontal direction to HOTMAC grid locations by using an inverse radius squared ($1/r^2$) interpolation method. Finally, the data were interpolated temporally to produce the hourly wind data.

The rawinsonde and wind profiler data were used to initialize the winds, potential temperatures, and mixing ratios of water vapor. The hourly interpolated data were used to nudge the HOTMAC predicted variables toward observations. Nudging was applied to the variables in the levels higher than 374 m above the ground. The variables in the layers below 374 m above the ground were computed by HOTMAC. The nudging coefficient used was 0.0005 s^{-1}, which is approximately five times larger than the Coriolis parameter.

The land use information included for this study was the land–water distributions. The water temperature was maintained at a constant value (15°C) throughout the simulations and the land temperatures were computed by solving a heat conduction equation for the soil layers, with the heat energy balance at the surface as the boundary condition (Yamada and Bunker 1988).

4. Results

a. Wind and turbulence

HOTMAC simulations started at 0400 MST 5 August 1992 (yearday 218) and ended at 1000 MST 17 August 1992 (yearday 230). The modeled wind vectors near the ground clearly displayed diurnal variations. During night, longwave radiative cooling resulted in lower temperatures over the sloped surfaces than those for the ambient air. This temperature difference generated horizontal pressure gradients and induced cold, dense airflows, which slid down the slopes to form valley drainage flows. Despite the fact that a relatively coarse grid spacing (4 km) was used because of limited computational resources, nocturnal drainage flows were well simulated (Fig. 2) along the Grand Canyon (GC) and the Colorado River Valley (CRV) (Fig. 1). On the other hand, wind vectors at higher levels were southwesterly and showed little variation in space (Fig. 3). The nocturnal drainage flows were confined to the shallow layer above the surface. During the day, upslope flows developed, directed toward the ridges along GC and CRV (Fig. 4). Upslope flows also were observed at higher levels, because strong vertical mixing from turbulence transported heat from the surface to substantially higher levels.

The modeled intensity of atmospheric turbulence also exhibited diurnal variations. In general, during night, atmospheric turbulence becomes small because the density stratification of the atmosphere is stable. For example, Fig. 5 shows the vertical profiles of the modeled standard deviation of vertical velocity (σ_w), twice the turbulence kinetic energy (q^2), and standard deviation of potential temperature (σ_Θ) at 0400 MST 6 August at Dolan Springs. For comparison, Fig. 6 shows the counterparts at 1400 MST. During the day, the atmosphere becomes unstable because of the heating from the ground, resulting in large turbulence, as seen in Fig. 6.

Wind direction, wind speed, and atmospheric turbulence vary with space and time because of differential heating and cooling over the sloped surfaces and influence from the large-scale weather variations. Wind and turbulence play critical roles for predicting the transport and diffusion of airborne materials.

b. Clouds

The modeled cloud distributions varied considerably with time and space. The modeled mixing ratios were nudged to the observed values. Observations at Cottonwood Cove indicated that relative humidity near the ground was less than 40% most of the time during the simulation period. Observed relative humidity exceeded 90% in the upper levels (3000–4000 m above the ground) at 0400 MST 5–6 August, at 1600 MST 8 August, and at 0400 MST 10 August. Thus, more clouds were generated during nighttime before the sunrise, and

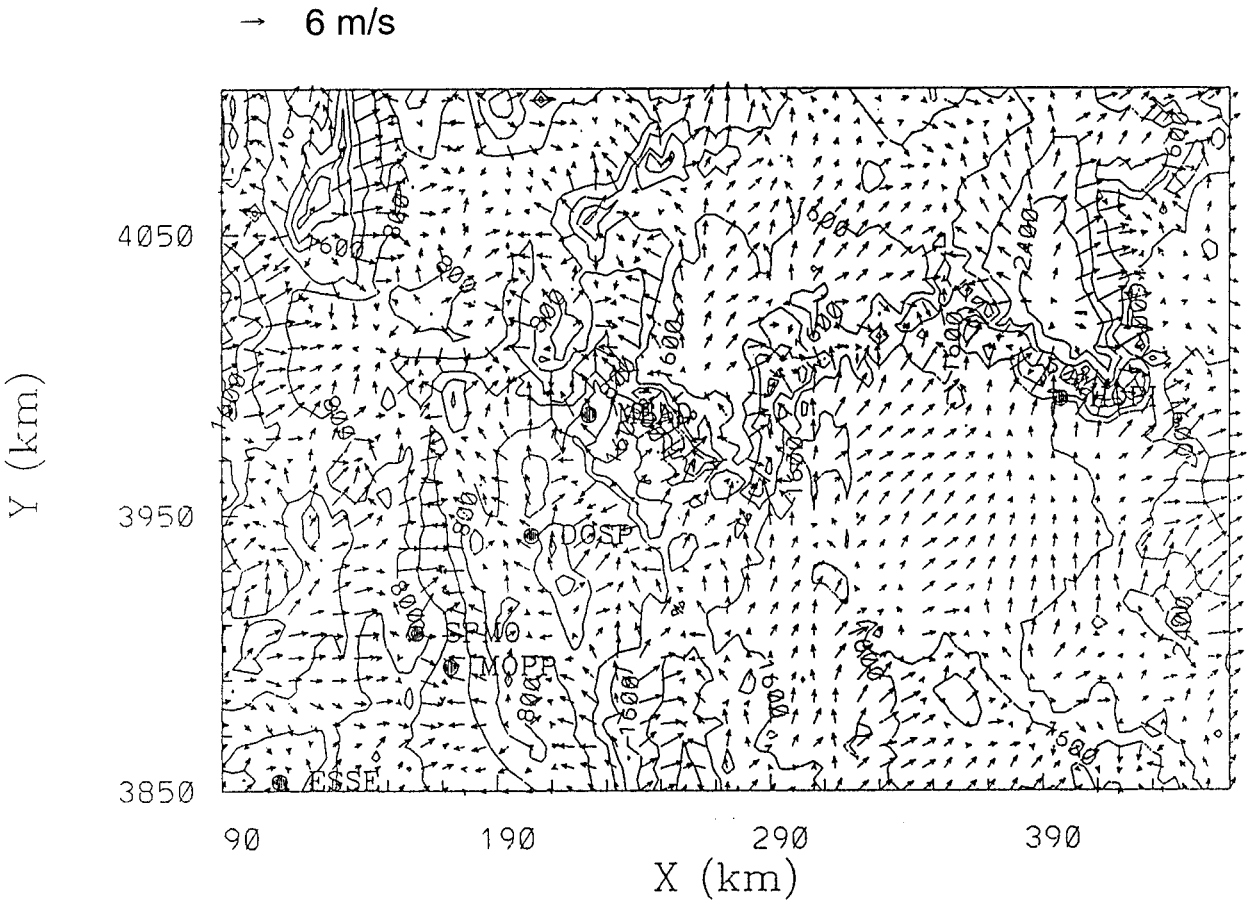

FIG. 2. The modeled wind distributions at 10 m above ground level (AGL) at 0400 MST on yearday 219 (6 Aug). Arrows indicate the wind directions, and the length of each arrow is proportional to the wind speed, the scale of which is indicated at the upper-left corner of the plot. Solid contour lines indicate ground elevation (m MSL), with an increment of 400 m between the contours. Locations of some stations also are indicated: Essex (ESSE), Mohave Power Project (MPP), Spirit Mountain (SPMO), Dolan Springs (DOSP), Meadview (MEAD), and Hopi Point (HOPO).

clouds dissipated during the daytime, although some convective clouds formed over the ridges.

HOTMAC computes cloud water mixing ratios, cloud coverage (the ratio of cloud volume to the grid volume), and second moments (turbulence fluxes) of cloud water mixing ratios. For example, Fig. 7 shows the vertical profiles of the modeled mixing ratio of total water (water vapor plus cloud water) and mixing ratio of cloud water at 0400 MST 6 August at MPP.

Cloud-base heights were determined from the vertical profiles of the modeled mixing ratio of cloud water (approximately 2300 m above the ground) as the lowest height at which the cloud water mixing ratio takes a small, nonzero value. No direct observation was made to determine the cloud-top and cloud-base heights. W. Moran and R. Farber (1997, personal communication) estimated cloud-base heights from the lifting condensation level (LCL) at Cottonwood Cove, Dolan Springs, and Page. The LCL is the height at which a parcel of air becomes saturated when it is lifted adiabatically. Temperature at the LCL was calculated from a formula that is a function of surface dewpoint and surface temperature. The altitude of the LCL then was determined from the soundings as the height at which the calculated temperature matches with the observation. Thus, the LCL is an estimate of cloud-base height but may not necessarily agree with the actual cloud height. Nevertheless, their LCL heights were in fair agreement with the modeled heights.

Cloud water supposedly decreases sharply at the cloud top in the atmosphere although there are no direct measurements. The modeled cloud water (Fig. 7) does not show such an abrupt decrease at the cloud top because the vertical grid spacing was too large (~300 m). Dynamical and physical effects resulting from modeled cloud water not matching with a generally observed cloud water profile at the cloud top are unknown because the computer capabilities and cost prohibited the increase in the vertical grid resolutions that is required for such sensitivity studies.

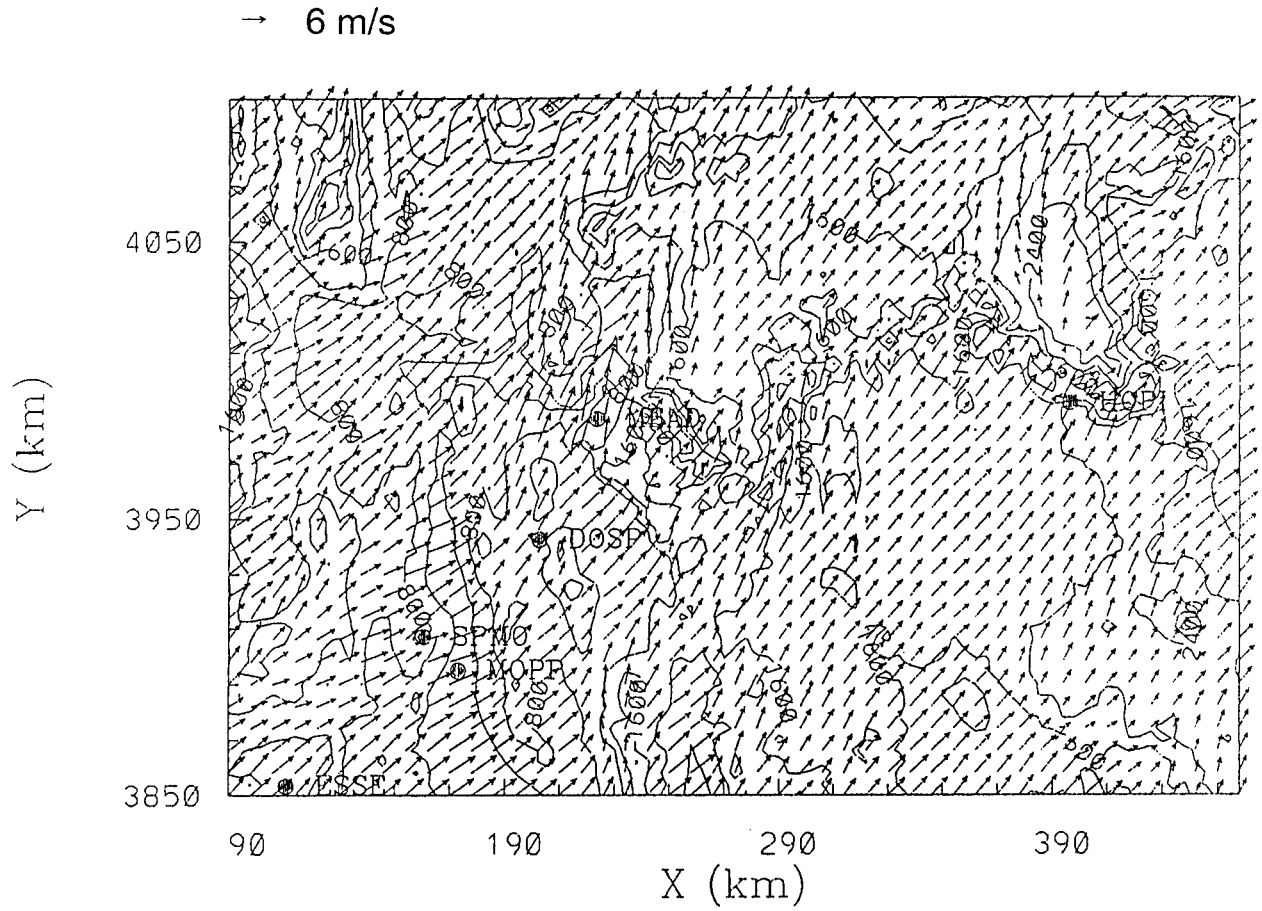

FIG. 3. Same as Fig. 2 but at 1056 m AGL.

Wind and turbulence distributions modeled by HOTMAC were used to compute transport and diffusion of tracer from MPP, as discussed in the following section. The modeled tracer concentrations and cloud distributions were used by other researchers for their chemical transformation modeling studies (Pitchford et al. 1999), which are not the subject of this paper.

c. Tracer release from MPP

During the 50-day summer intensive measurement period, from 12 July to 31 August 1992, tracer gas ocPDCH, ortho-cis-perfluorodimethylcyclohexane, was released continuously from MPP. The current study focuses on the 11-day period from 6 August to 17 August 1992. This particular period was chosen because a relatively large amount of tracer gas reached most of the sampling stations and available funding did not allow performance of simulations for the entire period.

Figure 8 shows hourly emission rates of oPDCH, of which 45% was ocPDCH, from MPP. These hourly emission rates were used in RAPTAD simulations. RAPTAD simulations started at 0400 MST 5 August 1992 (yearday 218) and ended at 0800 MST 17 August 1992 (yearday 230). RAPTAD simulation started 1 day earlier than the time for sampling initiation so that the modeled background concentration distributions are initialized to become similar to those of observations. The initial value of the vertical velocity used for solving Eq. (1) was 32 m s^{-1}, which was the observed emission velocity at the stack height (150 m above the ground). The initial value of the buoyancy used for solving Eq. (2) was 5 m s^{-1}, which was estimated by using Eq. (4) and the observed emission and ambient air temperatures at the stack exit. RAPTAD released puffs continuously from MPP and computed for each puff the center location, the standard deviations for the Gaussian concentration distribution, and the age counted from the release time. Large-scale wind directions were between southerly and southwesterly. Thus, puffs generally were transported in north to northeast directions, although wind directions varied considerably in the surface layers (Figs. 2 and 4).

Concentrations at ground level varied considerably with time. For example, the modeled concentrations at 0300 and 1400 MST 6 August 1992 are shown in Figs.

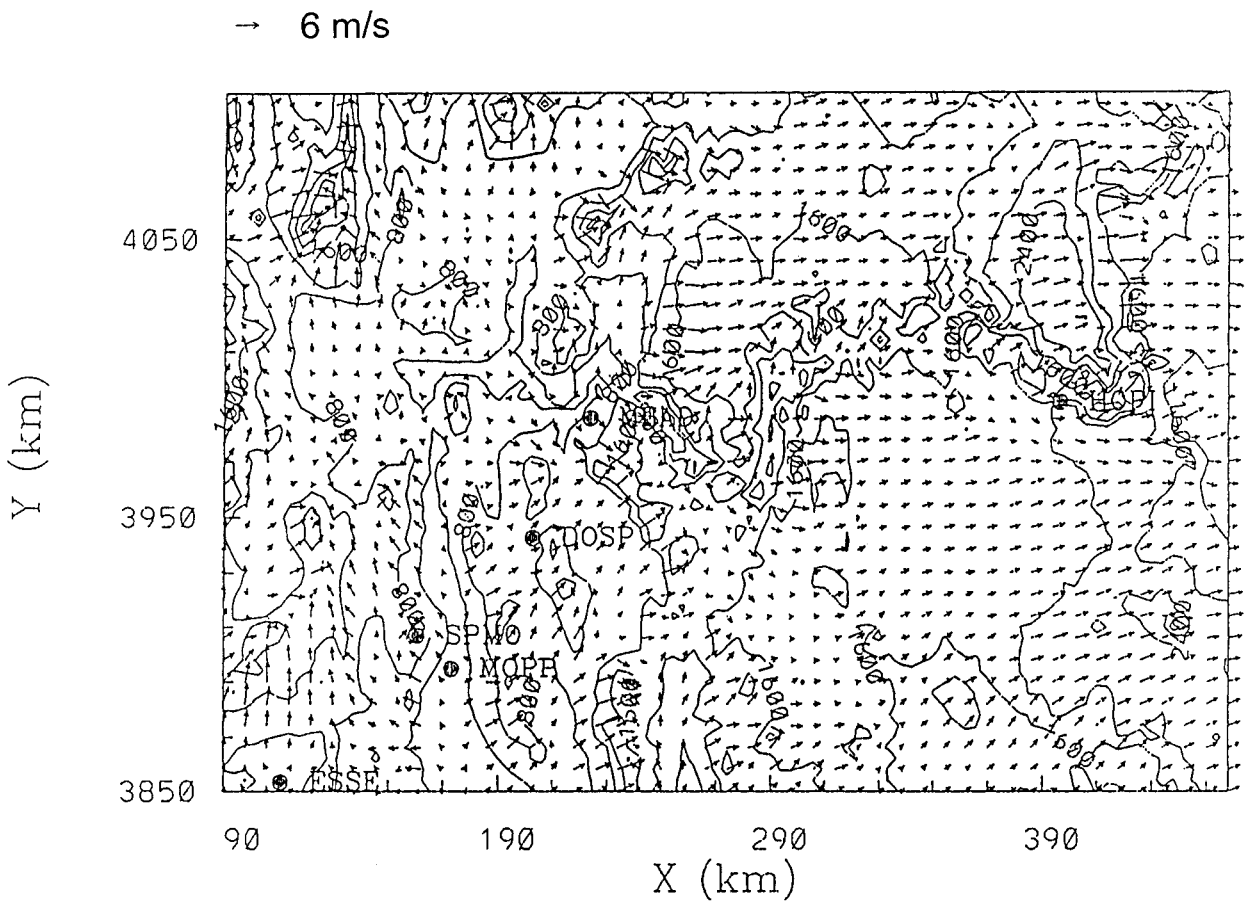

FIG. 4. Same as Fig. 2 but at 1400 MST.

9 and 10, respectively. Note that the concentration distributions are very different from the Gaussian distribution, although an individual puff is assumed to have a Gaussian concentration distribution.

Figure 11 shows time variations of modeled and observed concentrations of ocPDCH at selected receptors within the domain for the 11-day simulation period. The distances between the receptors and MPP source varied from several tens of kilometers to over 200 km. At Dolan Springs and Kingman, the modeled concentrations followed the temporal variations of the observations, resulting in relatively high correlation coefficients of 0.925 and 0.825, respectively. Furthermore, the modeled mean concentrations were within a factor of 2 of the observed mean concentrations (Table 1). Figure 11 shows that the model detected concentrations at Meadview with a bias of less than 2. However, statistical analyses indicated the correlation between the modeled and measured concentrations was not very good (0.337).

Table 1 presents a statistical summary of model performance at receptors within the computational domain. The mean concentrations, standard deviations, and coefficients of variation (standard deviation divided by mean) for both observations and predictions are listed. The bias (predicted mean divided by observed mean) and correlation coefficients also are presented, although the sample size is small for this short computation period. As shown in Table 1, the modeled surface concentration agrees well with the observations, as indicated by relatively small biases. The biases range between 0.631 and 2.243. Most biases fall within a factor of two, except for the receptor at Truxton (TRUX). The observed overall mean is 1.048 fl l^{-1} with a standard deviation of 2.754 fl l^{-1}. The modeled mean is 1.616 fl l^{-1} with a standard deviation of 2.063 fl l^{-1}. The overall performance of the model is satisfactory, with a bias of 1.542 and a correlation coefficient of 0.779.

d. Sensitivity study

In this section, the sensitivity of the modeled tracer concentration distributions to horizontal grid spacing is examined. The chosen horizontal grid spacing must be small enough to capture essential topographic features. Computational resources, on the other hand, do not always allow the chosen grid spacing to be as small as

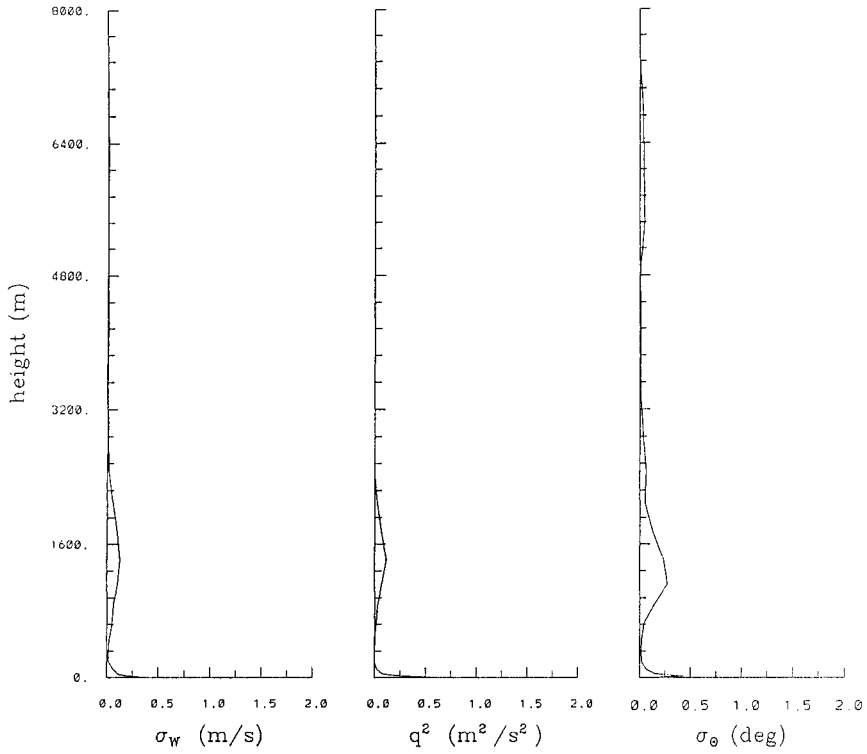

FIG. 5. Vertical profiles of the modeled standard deviation of vertical wind (σ_w), twice the turbulence kinetic energy (q^2), and standard deviation of potential temperature (σ_Θ) at 0400 MST on yearday 219 (6 Aug) at Dolan Springs.

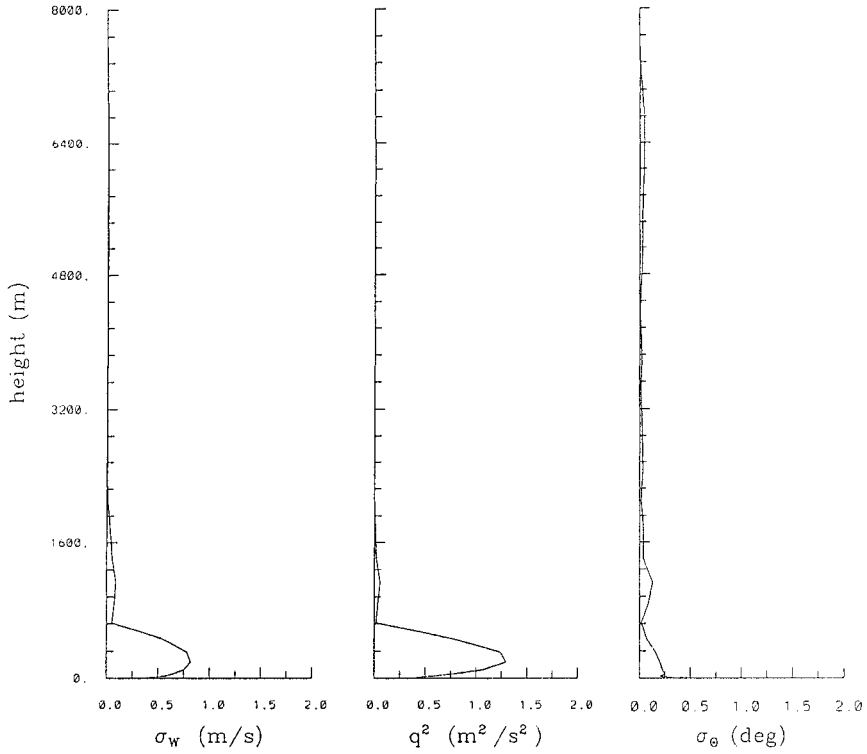

FIG. 6. Same as Fig. 5 but at 1400 MST.

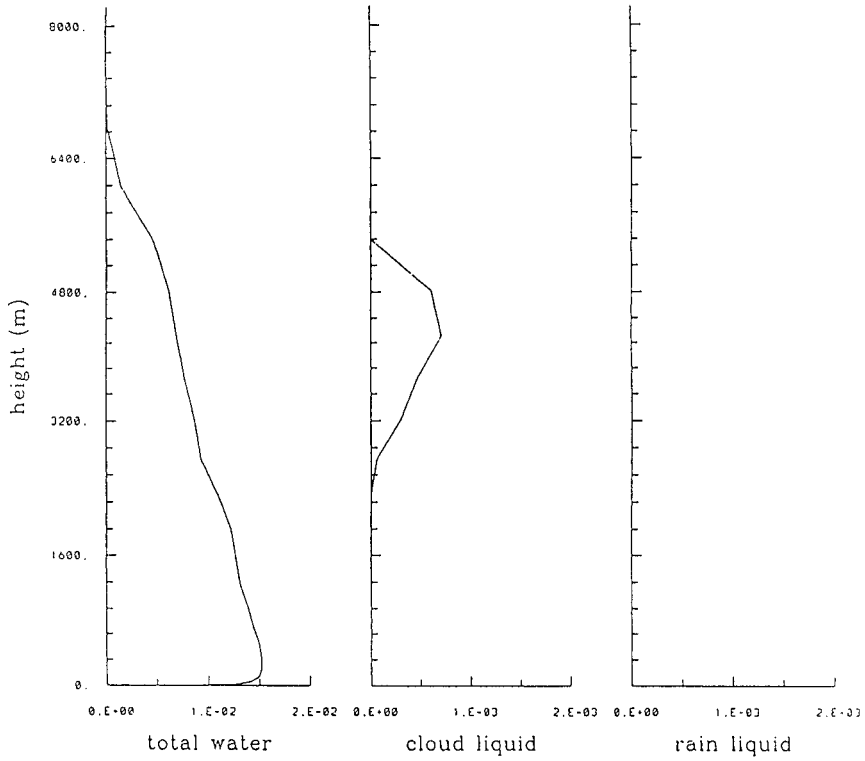

FIG. 7. Vertical profiles of the modeled mixing ratio of total water (water vapor plus cloud water) and cloud water (g g^{-1}) at 0400 MST on yearday 219 (6 Aug) at MPP. Computation for rainwater was turned off. Cloud-base heights were determined from the vertical profiles of cloud water mixing ratio.

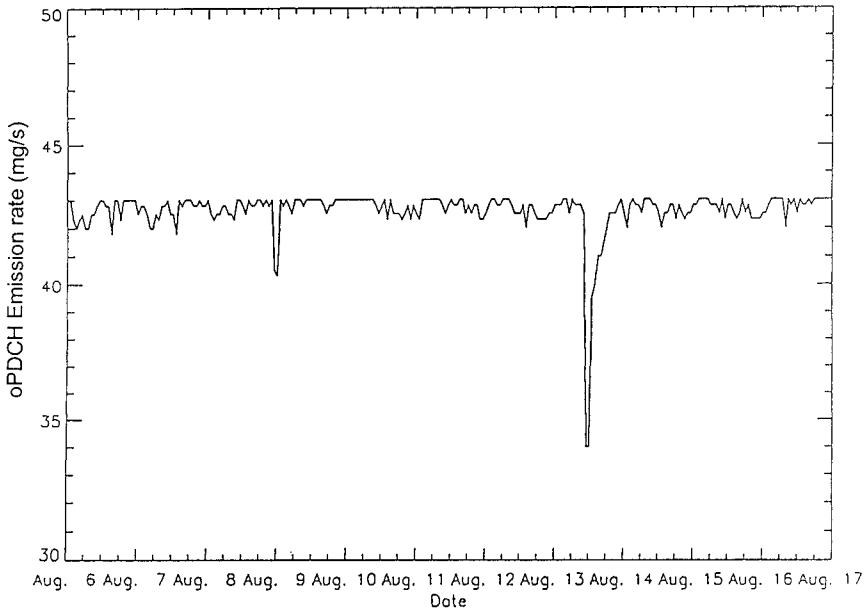

FIG. 8. Time variations of MPP oPDCH emission rate (mg s^{-1}) of which 45% is ocPDCH, for 6–17 Aug 1992. These emission rates were used as inputs to RAPTAD simulations.

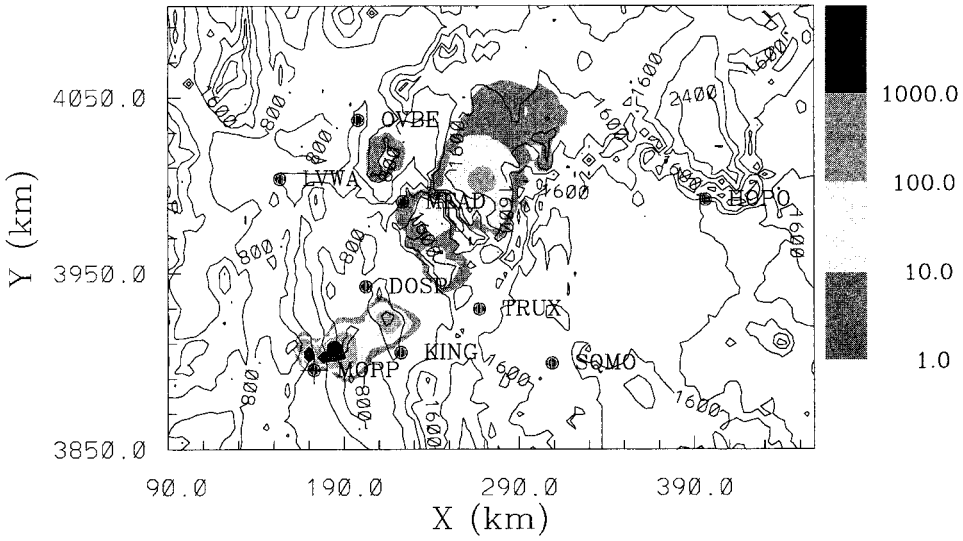

FIG. 9. The modeled surface concentration distributions (g m^{-3}) at 0300 MST 6 Aug 1992. Concentration scale bar is shown on the right-hand side of plot. The modeled concentration values were multiplied by 10^{12}. Solid contour lines indicate ground elevation (m MSL), with an increment of 400 m between the contours. Locations of some stations also are indicated: Mohave Power Project (MPP), Kingman (KING), Dolan Springs (DOSP), Las Vegas Wash (LVWA), Meadview (MEAD), Truxton (TRUX), Squaw Mountain (SQMO), and Hopi Point (HOPO).

desired. In the control run, a horizontal grid spacing of 4 km was used, which was the smallest value that could be used within the limitation of practicality. HOTMAC was rerun with a horizontal grid spacing of 12 km to examine the effect on the concentration distributions simulated by RAPTAD. The other conditions were the same as for the control run.

Figure 12 shows time variations of modeled and observed concentrations of ocPDCH at receptors within the study area for the 11-day simulation period. Figure 12 is the counterpart of Fig. 11 for the control run. The modeled overall mean is 1.800 fl l^{-1}(vs 1.616 for the control run) with a standard deviation of 1.490 fl l^{-1} (vs 2.063). The overall performance of the simulation is significantly lower than the control run, with a bias of 1.718 (vs 1.542) and a correlation coefficient of 0.323 (vs 0.779). It is, of course, expected that the results with a 12-km grid spacing will be poorer than those with a 4-km grid spacing. How much poorer was not known until simulations actually were performed.

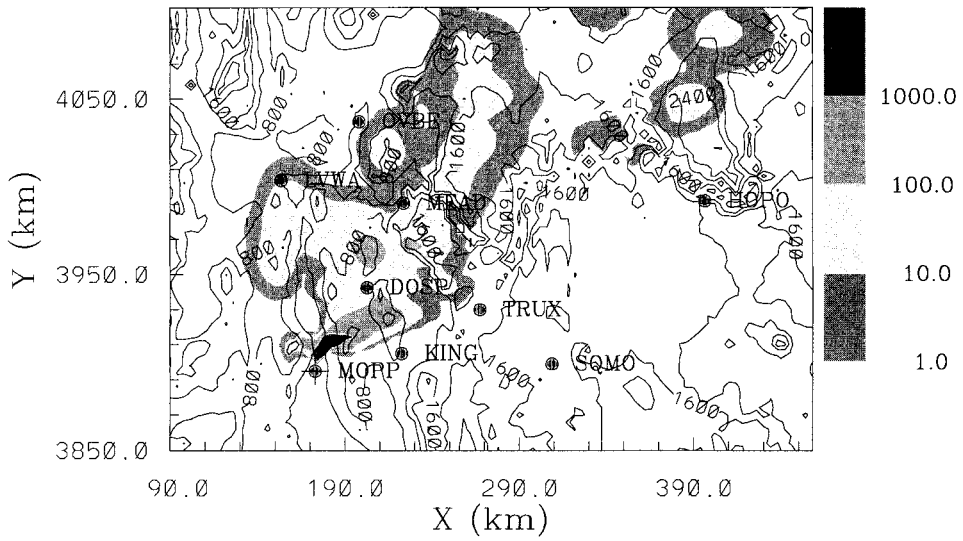

FIG. 10. Same as Fig. 9 but at 1400 MST 6 Aug 1992.

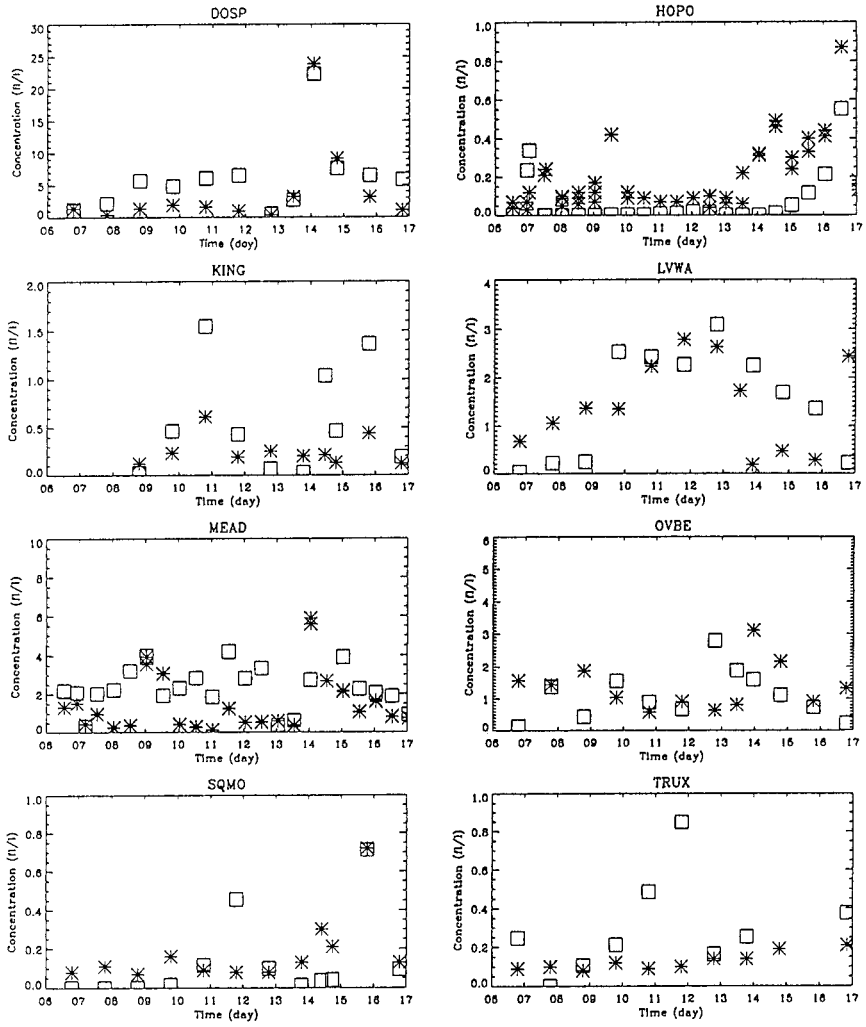

FIG. 11. Comparison between the observed (*) and modeled (□) concentrations (fl l^{-1}) at Dolan Springs (DOSP), Kingman (KING), Meadview (MEAD), Squaw Mountain (SQMO), Hopi Point (HOPO), Las Vegas Wash (LVWA), Overton Beach (OVBE), and Truxton (TRUX). Horizontal grid spacing of 4 km was used.

5. Summary

Three-dimensional atmospheric models, HOTMAC–RAPTAD, were used to simulate the wind and turbulence distributions and transport and diffusion of tracer gas for a portion of the summer intensive period of Project MOHAVE. With limited amounts of rawinsonde and wind profiler data, HOTMAC, with a horizontal grid spacing of 4 km (control run), was able to simulate qualitatively the diurnal variations of drainage and upslope flows along the Grand Canyon and the Colorado River Valley. HOTMAC also captured the diurnal variations of turbulence, which played important roles for the transport and diffusion simulations by RAPTAD.

The predicted ocPDCH surface concentrations agreed with actual measurement at Meadview to within a factor of 2, with a small standard deviation. Statistical analyses indicated that RAPTAD consistently predicted means within a factor of 2 of the measured means. The overall correlation coefficient of 0.779 indicated that RAPTAD has statistically meaningful prediction ability for long-distance transport and diffusion over complex terrain.

The sensitivity of the modeled tracer concentration distributions to horizontal grid spacing was examined. RAPTAD was rerun to simulate tracer data by using the wind and turbulence distributions simulated by a HOTMAC run in which a horizontal grid spacing of 12 km was used. The overall performance was significantly lower than it was for the control run, with a bias of 1.718 and a correlation coefficient of 0.323.

Acknowledgments. Simulations were assisted by Danny Lu, and the MOHAVE Project scientists provided

TABLE 1. Summary of model performance (sim = simulated; obs = observed). Coefficient of variance = standard deviation/mean; bias = simulated mean/observed mean. Site definitions are given in Fig. 11.

Station	Mean (fl L^{-1})	Standard deviation (fl L^{-1})	Coefficient of variance	Bias	Correlation coefficient
All_obs	1.048	2.754	2.629		
All_sim	1.616	2.063	1.277	1.542	0.779
DOSP_obs	4.087	1.470	0.360		
DOSP_sim	6.044	1.361	0.225	1.479	0.925
HOPO_obs	0.246	1.285	5.221		
HOPO_sim	0.155	1.789	11.524	0.631	0.174
KING_obs	0.302	1.101	3.646		
KING_sim	0.613	0.788	1.286	2.030	0.825
LVWA_obs	1.486	0.292	0.196		
LVWA_sim	1.938	1.022	0.527	1.304	0.246
MEAD_obs	1.397	1.305	0.934		
MEAD_sim	2.806	1.643	0.585	2.009	0.337
OVBE_obs	1.416	0.993	0.701		
OVBE_sim	1.168	0.774	0.663	0.825	−0.144
SQMO_obs	0.232	1.448	6.241		
SQMO_sim	0.184	1.288	6.994	0.794	0.715
TRUX_obs	0.261	1.539	5.893		
TRUX_sim	0.586	1.057	1.805	2.243	0.529

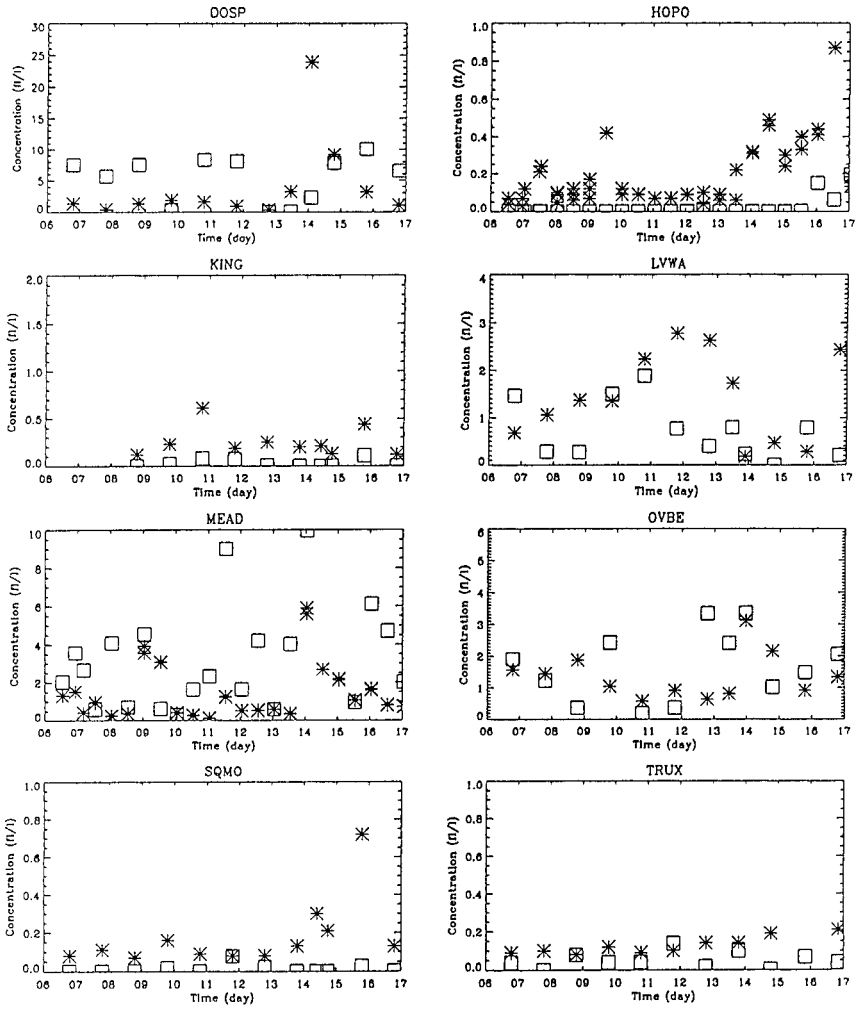

FIG. 12. Same as Fig. 11 but horizontal grid spacing of 12 km was used.

many useful comments during the course of the project. This Project MOHAVE–related work was supported by the Electric Power Research Institute under Contract W09156-02.

REFERENCES

Anthes, R. A., 1974: Data assimilation and initialization of hurricane prediction models. *J. Atmos. Sci.,* **31,** 702–719.

Green, M. C., 1997: Evaluation of atmospheric transport and dispersion models in highly complex terrain using perfluorocarbon tracer data. *Proc. 22d NATO/CCMS Int. Technical Meeting on Air Pollution Modeling and its Application*, Clermont-Ferrand, France, NATO/CCMS, 444–451.

Hoke, J. E., and R. A. Anthes, 1976: The initialization of numerical models by a dynamic-initialization technique. *Mon. Wea. Rev.*, **104,** 1551–1556.

Mellor, G. L., 1977: The Gaussian cloud model relations. *J. Atmos. Sci.,* **34,** 356–358.

——, and T. Yamada, 1982: Development of a turbulence closure model for geophysical fluid problems. *Rev. Geophys. Space Phys.,* **20,** 851–875.

Pitchford, M., M. Green, H. Kuhns, and R. Farber, 1997: Characterization of regional transport and dispersion using Project MOHAVE tracer data. *Proc. Visual Air Quality: Aerosols and Global Radiation Balance*, Bartlett, NH, Air and Waste Manage. Assoc., 181–200.

——, ——, ——, I. Tombach, W. Malm, M. Scruggs, R. Farber, and V. Mirabella, cited 1999: Project MOHAVE final report. [Available online at http://www.epa.gov./region09/air/mohave.html]

Van Dop, H., 1992: Buoyant plume rise in a Lagrangian framework. *Atmos. Environ.,* **26A,** 1335–1346.

Yamada, T., and G. L. Mellor, 1979: A numerical simulation of the BOMEX data using a turbulence closure model coupled with ensemble cloud relations. *Quart. J. Roy. Meteor. Soc.,* **105,** 915–944.

——, and C.-Y. J. Kao, 1986: A modeling study on the fair weather marine boundary layer of the GATE. *J. Atmos. Sci.,* **43,** 3186–3199.

——, and S. Bunker, 1988: Development of a nested grid, second moment turbulence closure model and application to the 1982 ASCOT Brush Creek data simulation. *J. Appl. Meteor.,* **27,** 562–578.

——, and ——, 1989: A numerical model study of nocturnal drainage flows with strong wind and temperature gradients. *J. Appl. Meteor.,* **28,** 545–554.